

# Luminescent Properties of (Sr, Zn)Al<sub>2</sub>O<sub>4</sub>:Eu<sup>2+</sup>, B<sup>3+</sup> Particles as a Potential Green Phosphor for UV LEDs

Kyeong Youl Jung,<sup>\*,†</sup> Hyun Woo Lee,<sup>‡</sup> and Ha-Kyun Jung<sup>‡</sup>

Department of Chemical Engineering, Kongju National University, Kongju, Chungnam, 314-701 Republic of Korea, and Advanced Materials Division, Korea Research Institute of Chemical Technology, 100, Jang-dong, Yuseong-gu, Daejeon, 305-343 Republic of Korea

Received January 2, 2006. Revised Manuscript Received March 9, 2006

(Sr<sub>1-x</sub>, Zn<sub>x</sub>)<sub>1-y</sub>(Al<sub>1.98</sub>, B<sub>0.02</sub>)O<sub>4</sub>:Eu<sup>2+</sup> green phosphor particles for ultraviolet light-emitting diodes (UV LEDs) were prepared by spray pyrolysis and their luminescent properties were investigated with changing the reducing temperature, the concentration of the activator, and the ratio of Sr to Zn. For the Sr(Al<sub>1.98</sub>, B<sub>0.02</sub>)O<sub>4</sub>:Eu<sup>2+</sup> phosphor, pure monoclinic SrAl<sub>2</sub>O<sub>4</sub> phase was formed when the post-treatment temperature was 1100–1200 °C. Over 1300 °C, however, the Sr<sub>4</sub>Al<sub>14</sub>O<sub>25</sub> phase appeared as a minor phase, which induced a blue shift in the emission peak. The highest intensity of Sr(Al<sub>1.98</sub>, B<sub>0.02</sub>)O<sub>4</sub>:Eu<sup>2+</sup> phosphor was achieved when the reducing temperature and the content of Eu<sup>2+</sup> were 1200 °C and 10 mol % of the strontium, respectively. It was found that the substitution of 10–50% Zn atoms instead of the strontium greatly enhanced the 520 nm green emission, especially for the excitation wavelength range from 380 to 420 nm. At the high Zn concentration ( $x > 0.7$ ), a new blue (460 nm) emission was observed and stable even at ambient temperature. This blue emission disappeared when the Zn content became lower than 0.7. The excitation spectrum of (Sr<sub>1-x</sub>, Zn<sub>x</sub>)(Al<sub>1.98</sub>, B<sub>0.02</sub>)O<sub>4</sub>:Eu<sup>2+</sup> phosphor ( $x \leq 0.7$ ) well overlapped with the 460 nm blue emissions. Consequently, it was concluded that the new blue sites successfully played the role of sensitizer for the energy transfer, which is responsible for the enhancement of the luminescence intensity. Finally, the optimized phosphor (Sr<sub>0.6</sub>, Zn<sub>0.4</sub>)<sub>0.9</sub>(Al<sub>1.98</sub>, B<sub>0.02</sub>)O<sub>4</sub>:Eu<sup>2+</sup><sub>0.1</sub> showed 185% improved emission intensity compared with that of the Sr<sub>0.9</sub>(Al<sub>1.98</sub>, B<sub>0.02</sub>)O<sub>4</sub>:Eu<sup>2+</sup><sub>0.1</sub> phosphor under ultraviolet ( $\lambda_{\text{ex}} = 393$  nm) excitation.

## 1. Introduction

The advent of GaN-based blue light-emitting diodes (LEDs) enables production of white light by means of combining various phosphors which can convert the blue light to green, yellow, and red.<sup>1–4</sup> In a comparison with the conventional incandescent and halogen lamps, the white-light generation through the blue LED combined with phosphor has many advantages such as low power consumption, long lifetime, and small size. Thus, many researchers are trying to develop a new light source with enhanced efficiency in order to save electrical energy, expecting substantial reduction in carbon-related pollution and creating a new optoelectronics-based lighting industry.<sup>5</sup>

YAG:Ce<sup>3+</sup> phosphor has been used as a yellow phosphor for GaN-based blue LED to make white light.<sup>6,7</sup> White LEDs

consisting of a blue GaN chip and YAG:Ce yellow phosphor, however, have a low color rendering index (CRI) and no full range of visible light. This drawback limits the expansion of LED application. One of the potential markets of white LEDs is backlight for liquid crystal displays (LCDs). Then, the backlight should have a full range of visible light as well as high brightness. The white light generated by combining a blue-LED chip and a yellow phosphor does not meet the requisition for LCD backlight. Therefore, it is necessary to develop a new strategy that generates the white light with high CRI and brightness. Recently, a suggested solution is to use a UV-diode with a primary emission of 370–410 nm instead of the blue LED.<sup>8–10</sup> That is, the UV LED chip is used as the excitation light and combined with red, green, and blue phosphors. To successfully generate the white LED through phosphor-combined UV LED, the phosphor materials should work under long-wavelength UV and have high emission efficiency. In this work, a potential green phosphor with high emission efficiency under the excitation of near-UV light (370–410 nm) was studied.

\* To whom correspondence should be addressed. E-mail: kyjung@kongju.ac.kr.  
Tel: +82-41-850-8640. Fax: +82-41-858-2575.

<sup>†</sup> Kongju National University.

<sup>‡</sup> Korea Research Institute of Chemical Technology.

(1) Nakamura, S.; Mukai, T.; Senoh, M. *Appl. Phys. Lett.* **1994**, *64*, 1687.

(2) Yang, W.-J.; Luo, L.; Chen, T.-M.; Wang, N.-S. *Chem. Mater.* **2005**, *17*, 3883.

(3) Yamada, M.; Naitou, T.; Zuno, K.; Tamaki, H.; Murazaki, Y.; Kameshima, M.; Mukai, T. *Jpn. J. Appl. Phys.* **2003**, *42*, L20.

(4) Kim, J. S.; Jeon, P. E.; Park, Y. H.; Choi, J. C.; Park, H. L. *Appl. Phys. Lett.* **2004**, *85*, 3696.

(5) Taso, J. Y., Ed. *Light Emitting Diodes (LEDs) for General Illumination Update 2002*; Optoelectronics Industry Development Association: Washington, DC, 2002.

(6) Schlotter, P.; Baur, J.; Hielscher, C.; Kunzer, M.; Obloh, H.; Schmidt, R.; Schneider, J. *Mater. Sci. Eng. B* **1999**, *59*, 390.

(7) Kasuya, R.; Isobe, T.; Kuma, H.; Katano, J. *J. Phys. Chem. B* **2005**, *109*, 22126.

(8) Li, Y. Q.; Delsing, A. C. A.; With, G. de; Hintzen, H. T. *Chem. Mater.* **2005**, *17*, 3242.

(9) Liao, Y.-C.; Lin, C.-H.; Wang, S.-L. *J. Am. Chem. Soc.* **2005**, *127*, 9986.

(10) Wang, T.; Liu, Y. H.; Lee, Y. B.; Ao, J. P.; Bai, J.; Sakai, S. *Appl. Phys. Lett.* **2002**, *81*, 2508.

Eu<sup>2+</sup>-doped MAI<sub>2</sub>O<sub>4</sub> (M = Sr, Ca) is well-known as a persistent phosphor.<sup>11,12</sup> SrAl<sub>2</sub>O<sub>4</sub>:Eu<sup>2+</sup> has the tridymite-like structure and good phosphorescence under UV irradiation,<sup>13</sup> but gives very low persistence. So the incorporation of Dy ion into the SrAl<sub>2</sub>O<sub>4</sub>:Eu<sup>2+</sup> is necessary to effectively enhance the long lasting phosphorescence as a consequence of forming a highly dense trapping level located at a suitable depth in relation to the thermal release rate at room temperature.<sup>14</sup> The SrAl<sub>2</sub>O<sub>4</sub>:Eu<sup>2+</sup>,Dy<sup>3+</sup>,B<sup>3+</sup> phosphor was reported by Murayama et al. to have enhanced phosphorescence. When a solid-state reaction is applied to prepare aluminates, boron oxide (B<sub>2</sub>O<sub>3</sub>) is used as a flux to accelerate grain growth.<sup>15</sup> According to previous studies,<sup>16,17</sup> the added B<sub>2</sub>O<sub>3</sub> is substituted in the AlO<sub>4</sub> framework of SrAl<sub>2</sub>O<sub>4</sub>, resulting in the enhancement of luminescence intensity at low concentration but the persistent phosphorescence suppressed with increasing the boron concentration. In the LED phosphor, the long persistent property is not necessary, but the enhanced luminescence intensity is needed. So we considered the SrAl<sub>2</sub>O<sub>4</sub>:Eu<sup>2+</sup>,B<sup>3+</sup> phosphor without the Dy coactivator as a potential green phosphor for UV-LED.

The optical properties of luminescent materials are frequently affected by the preparation method.<sup>18,19</sup> The particle size and the morphology of phosphors are also important variables, especially when a dense and thin phosphor layer should be formed or the phosphor handling process requires phosphor particles with fine size and spherical shape. The LED phosphor is well-mixed with epoxy resin and loaded on the LED chip by the nozzle dispensing process. Then, the phosphor particles with spherical shape and fine size are better than the irregular-shaped one. A solid-state reaction has been frequently used to study new compositional phosphor. The process requires a repetitive milling process to reduce the particle size. Nevertheless, the solid-state method yields relatively large particles of irregular shape. The aerosol processing, for example, spray pyrolysis, is known as a promising technique,<sup>20–24</sup> especially to prepare the multicomponent oxides such as the SrAl<sub>2</sub>O<sub>4</sub>:Eu<sup>2+</sup>,B<sup>3+</sup> phosphor. One particle is produced from one droplet. So the stoichiometry of multicomponent oxides can be controlled

easily. Moreover, the produced particles have spherical shape, fine size, and narrow size distribution.

In this work, highly luminous SrAl<sub>2</sub>O<sub>4</sub>:Eu<sup>2+</sup>,B<sup>3+</sup> particles with spherical shape and fine size were prepared by spray pyrolysis. First, we optimized the luminescence intensity of Sr(AI<sub>1.98</sub>, B<sub>0.02</sub>)O<sub>4</sub>:Eu<sup>2+</sup> particles under the excitation of UV light with changing the Eu<sup>2+</sup> concentration and the preparation temperature. To enhance the emission intensity, we tried to substitute zinc atoms for the strontium site and investigated the luminescent properties. Finally, it was found that the Zn substitution makes it possible to greatly enhance the photoluminescence of SrAl<sub>2</sub>O<sub>4</sub>:Eu<sup>2+</sup>,B<sup>3+</sup> phosphor.

## 2. Experimental Section

Strontium aluminates with composition (Sr<sub>1-x</sub>, Zn<sub>x</sub>)<sub>1-y</sub>(Al<sub>2-z</sub>, B<sub>z</sub>)O<sub>4</sub>:Eu<sup>2+</sup> (0 ≤ x ≤ 0.9, 0.005 ≤ y ≤ 0.15, z = 0.02) were prepared by spray pyrolysis. Sr(NO<sub>3</sub>)<sub>2</sub> (Aldrich, 99+%), Zn(NO<sub>3</sub>)<sub>2</sub>·6H<sub>2</sub>O (High Purity Co., 99.9%), Al(NO<sub>3</sub>)<sub>3</sub>·9H<sub>2</sub>O (Aldrich, 98+%), and H<sub>3</sub>BO<sub>3</sub> (Aldrich, 99.5+%) were used as the starting materials. These precursors were dissolved in water, wherein the total solution concentration was kept as 1.0 M. The nitrate solution prepared above was modified by the addition of NH<sub>4</sub>OH. Then the aluminum hydroxide molecules changed to polycations (Al<sub>x</sub>(OH)<sub>y</sub>(H<sub>2</sub>O)<sub>z</sub>)<sup>3x-y</sup>, in which the x and y depend on the concentration of aluminum hydroxide and pH of the solution (4.2–4.4 in this work).<sup>25</sup>

An ultrasonic aerosol generator with six vibrators (1.7 MHz) was used to atomize the precursor solution and the produced droplets were carried by air (45 L/min) into a hot furnace with a quartz tube (length, 1200 mm; inner diameter, 50 mm) at 900 °C. The formed particles were collected by a Teflon bag filter and post-treated at the temperature of 1000–1400 °C for 5 h under a reducing atmosphere (5% H<sub>2</sub>/N<sub>2</sub> mixture gas) for crystallization and activation of divalent europium. The crystal phase of the prepared particles was analyzed by an X-ray diffraction pattern measured by diffractometry (RIGAKU DMAX-33). The morphology was observed by scanning electron microscopy (SEM, Philips XL 30S FEG). The photoluminescence emission and excitation spectra of all samples were obtained with a spectrophotometer (Perkin-Elmer LS 50) using a Xe flash lamp.

## 3. Results and Discussion

Figure 1 shows X-ray diffraction patterns of Sr(AI<sub>1.98</sub>, B<sub>0.02</sub>)Eu<sup>2+</sup> particles. All the as-prepared particles have amorphous phase because the reaction temperature is low and the residence time (about 0.8 s in this work) of droplets or particles is too short to induce the crystallization. Thus, all samples were treated under a reducing atmosphere with changing the temperature from 1000 to 1400 °C. The particles had a hexagonal structure (JCPDS No. 31-1336, space group P6<sub>3</sub>22, a = 5.140 Å, c = 8.462 Å) at 1000 °C. When the post-treatment temperature was 1100–1200 °C, pure monoclinic SrAl<sub>2</sub>O<sub>4</sub> (JCPDS No. 34-0379, space group P2<sub>1</sub>, a = 8.447 Å, b = 8.816 Å, c = 5.163 Å, β = 93.42°) were formed. As the temperature became higher than 1300 °C, the major phase was monoclinic SrAl<sub>2</sub>O<sub>4</sub>, but Sr<sub>4</sub>Al<sub>14</sub>O<sub>25</sub> phase appeared as a minor phase. According to Nag and Kutty,<sup>17</sup> the formation of Sr<sub>4</sub>Al<sub>14</sub>O<sub>25</sub> is due to the reaction

- (11) Palilla, F.; Levine, A.; Momkus, M. *J. Electrochem. Soc.* **1968**, *115*, 642.
- (12) Blasse G.; Bril, A. *Philips Res. Rep.* **1968**, *23*, 201.
- (13) Ruiz-Gonzalez, M. L.; Gonzalez-Calbet, J. M.; valet-Regi, M.; Cordoncillo, E.; Escribano, P.; Carda, J. B.; Marchal, M. *J. Mater. Chem.* **2002**, *12*, 1128.
- (14) Matsuzawa, T.; Aoki, Y.; Takeuchi, N.; Murayama, Y. *J. Electrochem. Soc.* **1996**, *143*, 2670.
- (15) Murayama, Y.; Takeuchi, N.; Auki, Y.; Matsuzawa, T. U.S. Patent No. 5424006, 1995.
- (16) Niitykoski, J.; Aitasalo, T.; Hölsä, J.; Jungner, H.; Lastusaari, M.; Parkkinen, M.; Tukia, M. *J. Alloys Compd.* **2004**, *374*, 108.
- (17) Nag, A.; Kutty, T. R. N. *J. Alloys Compd.* **2003**, *354*, 221.
- (18) Cho, T. H.; Chang, H. J. *Ceram. Int.* **2003**, *29*, 611.
- (19) Lu, C.-H.; Hsu, W.-T.; Huang, C.-H.; Godbole, S. V.; Cheng, B.-M. *Mater. Chem. Phys.* **2005**, *90*, 62.
- (20) Jung, K. Y.; Lee, D. Y.; Kang, Y. C.; Park, H. D. *J. Lumin.* **2003**, *105*, 127.
- (21) Kang, Y. C.; Roh, H. S.; Park, H. D.; Park, S. B. *Ceram. Int.* **2003**, *29*, 41.
- (22) Jung, K. Y.; Kim, E. J.; Kang, Y. C. *J. Electrochem. Soc.* **2004**, *151*, H69.
- (23) Shimomura, Y.; Kijima, N. *J. Electrochem. Soc.* **2004**, *151*, H192.
- (24) Jeoung, B. W.; Hong, G. Y.; Yoo, W. T.; Yoo, J. S. *J. Electrochem. Soc.* **2004**, *151*, H213.

- (25) Brinker, C. J.; Scherer, G. W. *Sol-Gel Science*; Academic Press: New York, 1990.

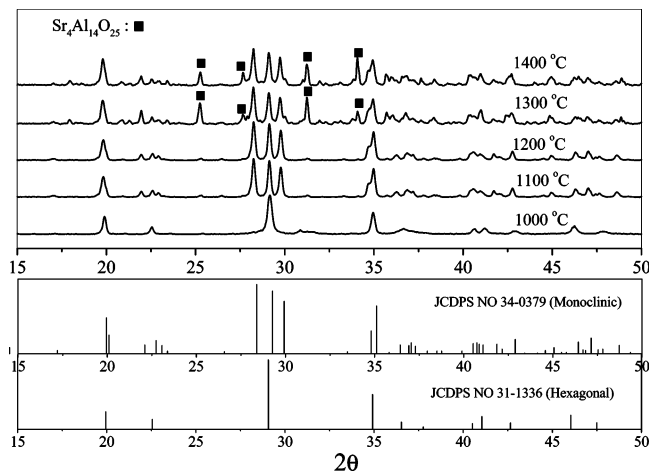


**Figure 1.** Dependence of XRD patterns on the reducing temperature for  $\text{Sr}(\text{Al}_{1.98}, \text{B}_{0.02})\text{O}_4:\text{Eu}^{2+}$  particles.

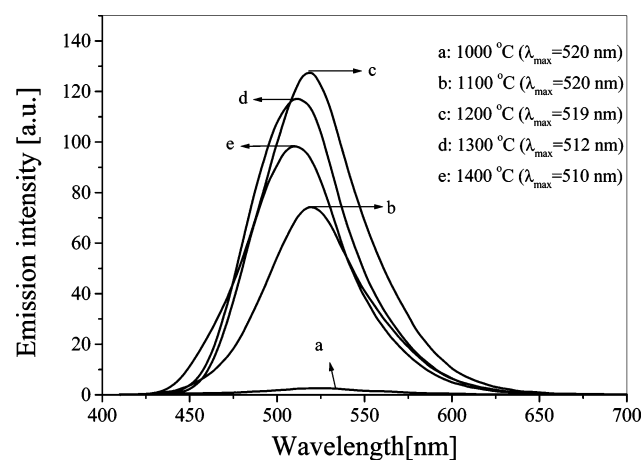


**Figure 2.** Emission spectra of prepared strontium aluminates at several temperatures ( $\lambda_{\text{ex}} = 393 \text{ nm}$ ).

of  $\text{B}_2\text{O}_3$  and  $\text{SrAl}_2\text{O}_4$ . They reported that  $\text{SrAl}_2\text{B}_2\text{O}_7$  cubic or hexagonal phase is formed at high  $\text{B}_2\text{O}_3$  concentration. In this work, the boron content was not high. As a result, there was no peak for the  $\text{SrAl}_2\text{B}_2\text{O}_7$  cubic or hexagonal phase even at  $1400 \text{ }^\circ\text{C}$ .

Figure 2 shows the effect of the post-treatment temperature on the emission spectrum of the prepared  $\text{Sr}(\text{Al}_{1.98}, \text{B}_{0.02})\text{O}_4:\text{Eu}^{2+}$  particles. The particles with hexagonal phase showed a very weak photoemission, whereas all the monoclinic phase had an intensive green emission. A blue shift in the emission spectrum of  $\text{Sr}(\text{Al}_{1.98}, \text{B}_{0.02})\text{O}_4:\text{Eu}_{0.1}$  particles was observed with increasing the post-treatment temperature. The broad emission results from the  $4f^7(^8\text{S})-4f^65d^1$  transition of  $\text{Eu}^{2+}$ , which strongly depends on the crystal field symmetry of the host lattice.<sup>26,27</sup> That is, the excited state involving the 5d orbital is split in a different level by changing the crystal field strength, which results in the different emission color. It was reported that pure  $\text{SrAl}_2\text{O}_4$  phase has the emission peak at  $520 \text{ nm}$ , whereas pure  $\text{Sr}_4\text{Al}_{14}\text{O}_{25}$  phase shows the emission centered at  $490 \text{ nm}$ .<sup>28,29</sup> As shown in Figure 1,  $\text{Sr}_4$ -

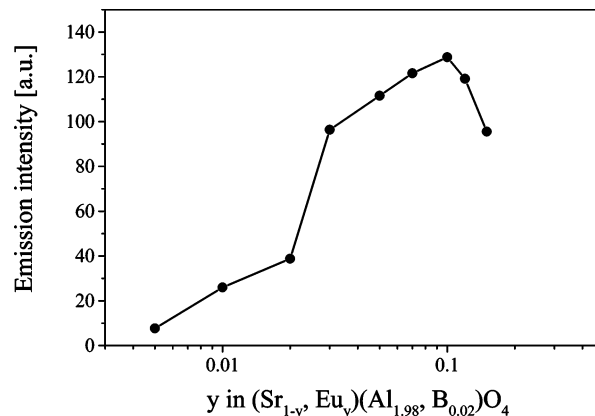


**Figure 3.** Emission intensity of strontium aluminates as a function of the  $\text{Eu}^{2+}$  concentration.

$\text{Al}_{14}\text{O}_{25}$  phase appeared as a minor phase when the post-treatment temperature was over  $1300 \text{ }^\circ\text{C}$ . Therefore, the blue shift in the emission spectrum of  $\text{Sr}(\text{Al}_{1.98}, \text{B}_{0.02})\text{O}_4:\text{Eu}_{0.1}$  particles is channeled into the change of the crystal field strength by the formation of  $\text{Sr}_4\text{Al}_{14}\text{O}_{25}$  phase with increasing the post-treatment temperature. Finally, the optimal temperature, giving the highest luminescence intensity, was  $1200 \text{ }^\circ\text{C}$ . So, for the following phosphor, the reducing temperature was fixed at  $1200 \text{ }^\circ\text{C}$ .

The luminescence intensity of the phosphor is strongly influenced by the activator concentration.<sup>30,31</sup> When considering an ideal situation where there is no concentration quenching, the emission intensity should be proportional to the number of  $\text{Eu}^{2+}$  existing within the layer to which the UV light reaches. But there is always a critical concentration, which is defined as the concentration at which the emission intensity begins to decrease. The optimal  $\text{Eu}^{2+}$  content also depends on the preparation method. Thus, the critical concentration of  $\text{Eu}^{2+}$  ions was experimentally studied to optimize the photoluminescence of the  $\text{Sr}(\text{Al}_{1.98}, \text{B}_{0.02})\text{O}_4:\text{Eu}^{2+}$  particles when they are prepared by spray pyrolysis. Figure 3 shows the emission intensity of prepared strontium aluminates as a function of the  $\text{Eu}^{2+}$  concentration. The highest intensity was observed when the content of  $\text{Eu}^{2+}$  was 10 mol % ( $y = 0.1$  in Figure 3). Thus, the content of  $\text{Eu}^{2+}$  was fixed at 10 mol %.

The codopant  $\text{B}^{3+}$  ions is substituted for the  $\text{Al}^{3+}$  sites, which is proved by IR and NMR measurement.<sup>17</sup> According to Clabau et al.,<sup>32</sup> an increase in the concentration of oxygen vacancies by codoping with  $\text{B}^{3+}$  is responsible for the improvement of photoluminescence. It was also reported that  $\text{B}_2\text{O}_3$  induces the phase transformation from  $\text{SrAl}_2\text{O}_4$  to  $\text{Sr}_4\text{Al}_{14}\text{O}_{25}$ .<sup>17</sup> Thus, a large content of boron does not increase but decrease the photoluminescence because the luminescent intensity of  $\text{Sr}_4\text{Al}_{14}\text{O}_{25}:\text{Eu}^{2+}$  is lower than that of  $\text{SrAl}_2\text{O}_4:\text{Eu}^{2+}$  when they are prepared by spray pyrolysis. So we checked whether the codopant  $\text{B}^{3+}$  enhances the photolu-

(26) Perkowitz, S. *Optical Characterization of Semiconductors; Infrared, Raman, and Photoluminescence Spectroscopy*; Academic Press: New York, 1993.  
 (27) Dorenbos, P. *J. Lumin.* **2003**, *104*, 239.  
 (28) Smets, B.; Rutten, J.; Hoeks, G.; Verlijsdonk, J. *J. Electrochem. Soc.* **1989**, *13*, 2119.

(29) Nag, A.; Kutty, T. R. N. *Mater. Res. Bull.* **2004**, *39*, 331.  
 (30) Yu, M.; Lin, J.; Wang, Z.; Fu, J.; Wang, S.; Zhang, H. J.; Han, Y. C. *Chem. Mater.* **2002**, *14*, 2224.  
 (31) Kim, K.-B.; Kim, Y.-I.; Chun, H.-G.; Cho, T.-Y.; Jung, J.-S.; Kang, J.-G. *Chem. Mater.* **2002**, *14*, 5045.  
 (32) Clabau, F.; Rocquefelte, X.; Jobic, S.; Deniard, P.; Whangbo, M.-H.; Garcia, A.; Le Mercier, T. *Chem. Mater.* **2005**, *17*, 3904.



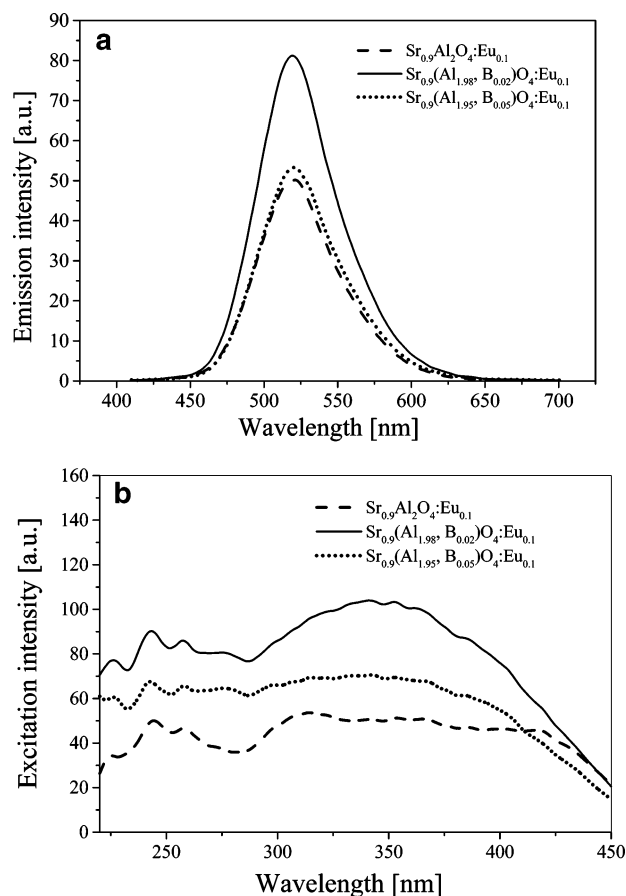


**Figure 4.** Emission (a) and excitation (b) spectra of  $\text{SrAl}_2\text{O}_4:\text{Eu}^{2+}$  and  $\text{Sr}(\text{Al}_{2-z}, \text{B}_z)\text{O}_4:\text{Eu}^{2+}$  phosphor ( $\lambda_{\text{ex}} = 395 \text{ nm}$  and  $\lambda_{\text{em}} = 520 \text{ nm}$ ).

minescence or not. Figure 4 shows the emission and excitation spectra of  $\text{Sr}_{0.9}(\text{Al}_{2-z}, \text{B}_z)\text{O}_4:\text{Eu}^{2+}_{0.1}$  particles, wherein  $z$  was changed as 0.02 and 0.05, respectively. It was clear that the substitution of boron was helpful for increasing the luminescent intensity. The increase of the luminescent intensity, however, was weakened when the fraction of boron was 0.05. According to the XRD analysis, more  $\text{Sr}_4\text{Al}_{14}\text{O}_{25}$  phase was formed at  $z = 0.05$  compared with  $z = 0.02$ . So it was confirmed that increasing the boron content accelerates the formation of  $\text{Sr}_4\text{Al}_{14}\text{O}_{25}$  phase, which is responsible for weakening the positive effect of boron on the photoluminescence. The phosphor for the UV LEDs should have a good excitation spectrum in the wavelength from 370 to 410 nm. As shown in Figure 4, the codoping of  $\text{B}^{3+}$  ( $z = 0.02$ ) greatly enhanced the excitation property in the wavelength of shorter than 400 nm. From the results so far achieved, it was confirmed that the codoping of  $\text{B}^{3+}$  is helpful and necessary to improve the luminescence of strontium aluminates under the long-wavelength UV illumination.

When the spray pyrolysis is used to prepare the phosphor materials, one of the advantages is production of a spherical phosphor with fine size. The spray pyrolysis, however, frequently produces hollow-structured particles because the precipitation of ingredients begins first at the surface of the droplets due to the fast evaporation of water passing through a hot furnace. Then the hollow particles collapsed and agglomerated during the post heat treatment. As a result, the spherical shape could not be maintained. To avoid this bad situation, the properties of the spray solution should be

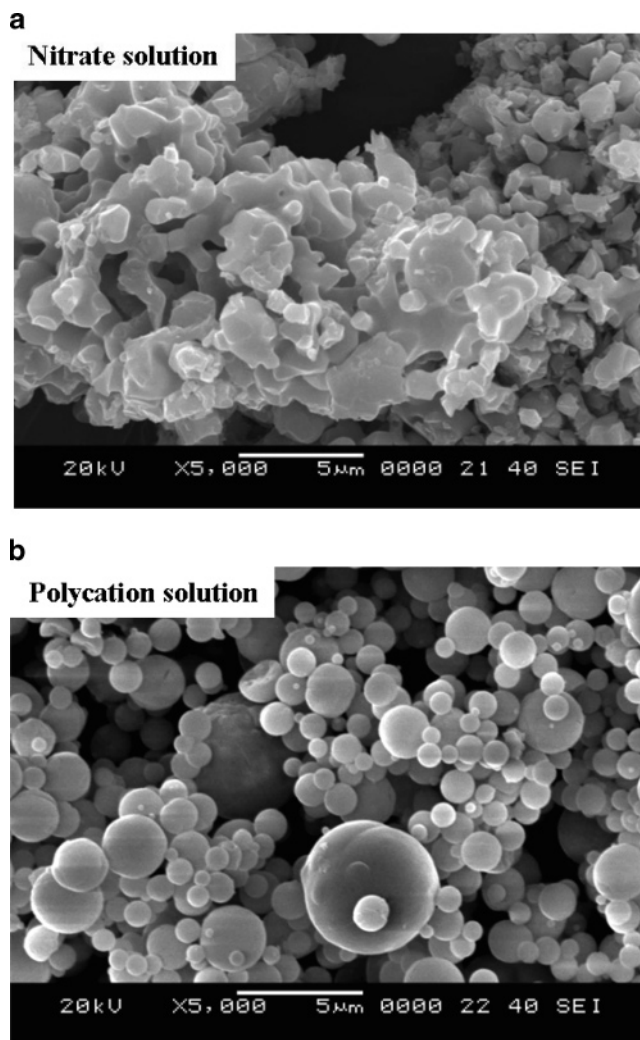


**Figure 5.** SEM photos of strontium aluminates prepared by spray pyrolysis from the solution of nitrate (a) and polycation (b).

changed, to induce the volumetric precipitation rather than the local one. In a previous study,<sup>33,34</sup> we proposed a solution technique that makes it possible to obtain solid phosphor particles when the spray pyrolysis is applied to prepare barium magnesium aluminates ( $\text{BaMgAl}_{10}\text{O}_{17}$ ). The same solution technique was applied to prepare the strontium aluminates. The nitrate precursors were dissolved in purified water, which is called “nitrate solution”. This nitrate solution was modified by the addition of  $\text{NH}_4\text{OH}$  to obtain aluminum polycations.<sup>25</sup> Figure 5 shows SEM photos of  $\text{Sr}_{0.9}(\text{Al}_{1.98}, \text{B}_{0.02})\text{O}_4:\text{Eu}^{2+}$  particles which were thermally treated at  $1200^\circ\text{C}$  for 5 h. The particles prepared from the nitrate solution were agglomerated and did not have spherical shape because the as-prepared particles had a hollow structure, whereas the particles prepared from the polycation solution had spherical shape, which means that the as-prepared particles are not hollow but solid. The aluminum polycations in droplets easily induce the gelation when the concentration increases by evaporating the water in a hot furnace. Thereby, the local precipitation is inhibited and the volume precipitation occurs.

(33) Lee, D. Y.; Kang, Y. C.; Jung, K. Y. *Electrochem. Solid-State Lett.* **2003**, *6*, H27.

(34) Jung, K. Y.; Lee, H. W.; Kang, Y. C.; Park, S. B.; Yang, Y. S. *Chem. Mater.* **2005**, *17*, 2729.

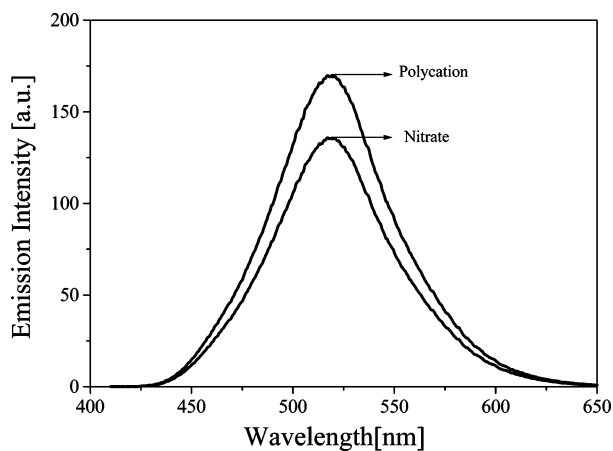


**Figure 6.** Emission spectra of strontium aluminates prepared by spray pyrolysis from the solution of nitrate (a) and polycation (b).

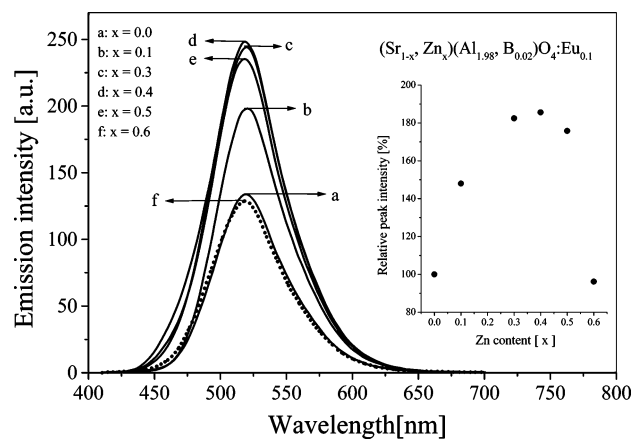


**Figure 7.** Emission spectra of  $(\text{Sr}_{1-x}, \text{Zn}_x)(\text{Al}_{1.98}, \text{B}_{0.02})\text{O}_4:\text{Eu}^{2+}$  phosphor ( $\lambda_{\text{ex}} = 393$  nm).

As a result, solid particles were produced. The particle morphology influences the photoluminescence intensity as shown in Figure 6. The spherical particles prepared from the polycation solution showed higher photoluminescence intensity compared with that of the irregular-shaped particles.

To improve the luminescence intensity, an attempt was made to replace strontium with zinc. Figure 7 shows the emission spectra of  $(\text{Sr}_{1-x}, \text{Zn}_x)_{0.9}(\text{Al}_{1.98}, \text{B}_{0.02})\text{O}_4:\text{Eu}^{2+}_{0.1}$  particles which were prepared from the polycation solution. All spectra were measured by the illumination of UV ( $\lambda_{\text{ex}} = 393$  nm) light. The emission intensity was remarkably enhanced until the content of zinc increased up to 40% ( $x = 0.4$ ). When the content of zinc was over 60%, however, the emission intensity was much lower than that of  $\text{Sr}_{0.9}(\text{Al}_{1.98}, \text{B}_{0.02})\text{O}_4:\text{Eu}^{2+}_{0.1}$  particles. The highest intensity at  $x = 0.4$  was about 185% higher than that of the  $\text{Sr}_{0.9}(\text{Al}_{1.98}, \text{B}_{0.02})\text{O}_4:\text{Eu}^{2+}_{0.1}$  particles. It is notable that the maximum peak position of the emission band was not changed until the content of zinc atoms was 70% ( $x = 0.7$ ). As mentioned before, the emission of  $\text{Eu}^{2+}$  is highly dependent on the crystal field strength. The addition of Zn can change the surroundings of  $\text{Eu}^{2+}$  and the crystal structure. Then some different emission sites can be formed. This postulation was identified from the samples in which the zinc content was higher than 80% ( $x = 0.8$  and  $0.9$ ). Figure 8 shows the emission spectra of the samples prepared at the zinc content of higher than 80%. When 100% strontium was substituted

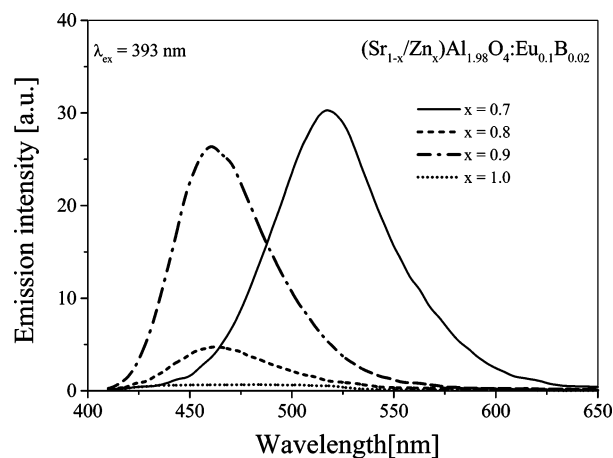


**Figure 8.** Dependence of the emission spectrum on the content of Zn atoms for  $(\text{Sr}_{1-x}, \text{Zn}_x)(\text{Al}_{1.98}, \text{B}_{0.02})\text{O}_4:\text{Eu}^{2+}$  phosphor.

with zinc, no emission peak was observed under the UV ( $\lambda_{\text{ex}} = 393$  nm) illumination. A new peak, however, appears at 460 nm in the samples for  $x = 0.8$  and  $0.9$ . The sites for dopants in the host are determined by their ionic radii. The radius of  $\text{Eu}^{2+}$ ,  $\text{Sr}^{2+}$ , and  $\text{Zn}^{2+}$  is 0.120, 0.121, and 0.083 nm, respectively. Thus, the  $\text{Eu}^{2+}$  ions can readily occupy the  $\text{Sr}^{2+}$  sites rather than the  $\text{Zn}^{2+}$  sites. For the samples in which the content of zinc is 80–90%, the  $\text{Eu}^{2+}$  ions occupy the  $\text{Sr}^{2+}$  sites. Such a significant addition of Zn, whose size is much smaller than Sr, leads to some shrinkage of the lattice. This will exert larger crystal field on the Eu dopant. Therefore, the 460 nm emission ( $\lambda_{\text{ex}} = 393$  nm) for the  $x = 0.8$  and  $0.9$  samples results from the  $4f^65d^1 \rightarrow 4f^7(^8S_{7/2})$  transition of  $\text{Eu}^{2+}$  ions located at the  $\text{Sr}^{2+}$  sites.

Poort et al. reported the  $\text{SrAl}_2\text{O}_4:\text{Eu}$  phosphor has an additional emission peak at 450 nm when the measuring temperature is 4.5 K.<sup>35</sup> They suggested that the 450 nm emission also originates from the  $4f^65d^1 \rightarrow 4f^7(^8S_{7/2})$  transition of  $\text{Eu}^{2+}$  located at a strontium site which is different from the site for the 520 nm emission. At room temperature, however, the 450 nm peak disappears. Thus, it is surmised that the 460 nm emission for the  $x = 0.8$  and  $0.9$  samples arises not from the same sites reported in the literature for the 450 nm emission of  $\text{SrAl}_2\text{O}_4:\text{Eu}^{2+}$ ,<sup>35</sup> but from new emission sites that are stable at ambient temperature. These new emission sites seem to be produced by replacing the Sr site with the Zn atom. As the zinc content decreased, the green emission was dominated (see the  $x = 0.7$  sample in Figure 8). One interesting finding was that only one peak, either 460 or 520 nm, was observed in all the samples ( $x = 0.0$ – $1.0$ ). The 520 nm emission is obviously due to the  $4f^65d^1 \rightarrow 4f^7(^8S_{7/2})$  transition of  $\text{Eu}^{2+}$  located at a strontium site in the  $\text{SrAl}_2\text{O}_4$  phase. According to the XRD results shown in Figure 9, the monoclinic  $\text{SrAl}_2\text{O}_4$  still remained as a major phase even when the Zn content ( $x$ ) goes up to 0.7. When the Zn content ( $x$ ) was over 0.8, however, the zinc aluminates became a dominant crystal phase, whereas the  $\text{SrAl}_2\text{O}_4$  phase existed as a minor one. On the basis of XRD and photoluminescence results,  $(\text{Sr}_{1-x}, \text{Zn}_x)_{0.9}(\text{Al}_{1.98}, \text{B}_{0.02})\text{O}_4:\text{Eu}^{2+}_{0.1}$  phosphor appeared to have the green emission at 520 nm if

(35) Poort, S. H. M.; Blokpoel, W. P.; Blass, G. *Chem. Mater.* **1995**, *7*, 1547.

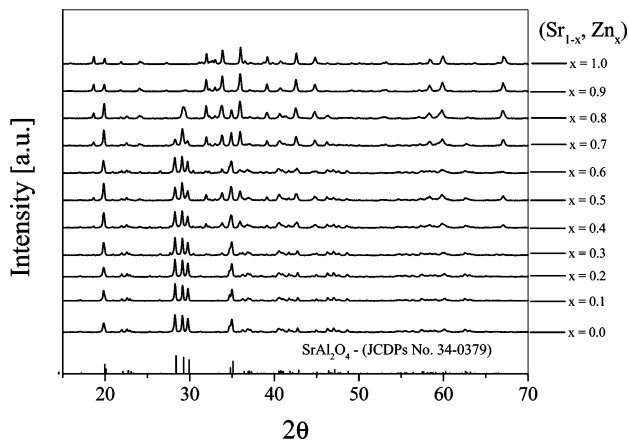


Figure 9. XRD patterns of  $(\text{Sr}_{1-x}, \text{Zn}_x)(\text{Al}_{1.98}, \text{B}_{0.02})\text{O}_4:\text{Eu}^{2+}$  phosphor.

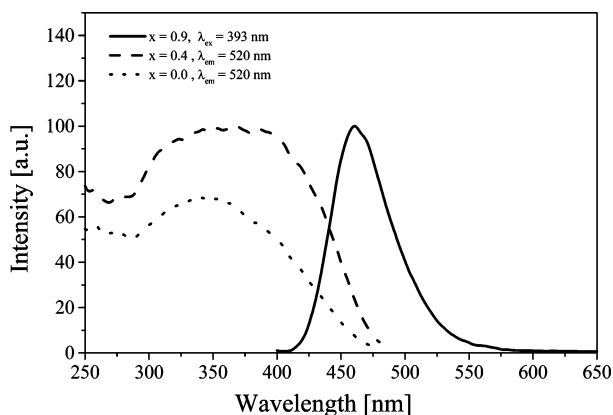


Figure 10. Emission spectrum of  $(\text{Sr}_{0.1}, \text{Zn}_{0.9})(\text{Al}_{1.98}, \text{B}_{0.02})\text{O}_4:\text{Eu}^{2+}$  and excitation spectra of  $(\text{Sr}_{0.6}, \text{Zn}_{0.4})(\text{Al}_{1.98}, \text{B}_{0.02})\text{O}_4:\text{Eu}^{2+}$  and  $\text{Sr}(\text{Al}_{1.98}, \text{B}_{0.02})\text{O}_4:\text{Eu}^{2+}$  samples.

the phosphor has the monoclinic  $\text{SrAl}_2\text{O}_4$  phase as the major crystal phase. The significant changes in the structure for the samples in which the Zn content ( $x$ ) is over 0.8 lead to the change in the crystal field strength, exerting the  $\text{Eu}^{2+}$  dopants, which directly affects the luminescent property. These changes are well-correlated with the appearance of the 460 nm emission.

For the samples in which the zinc content ( $x$ ) is lower than 0.7, the luminescent sites for the 460 and 520 nm emissions should coexist. However, no peak at 460 nm was observed in the samples with the Zn content lower than 0.7. The disappearance of the 460 nm emission and the enhancement of the 520 nm emission support the belief that there is an energy transfer from the sites for the 460 nm emission to the sites for the 520 nm one. It is well-known that the energy transfer from a sensitizer to an activator occurs when the emission band of the sensitizer overlaps with the absorption of the activator.<sup>36</sup> That is, the sites for the 460 nm emission play the role of sensitizer and effectively transfer the energy to the sites for the 520 nm emission. To satisfy this postulation, the excitation band of the  $\text{Sr}_{0.9}(\text{Al}_{1.98}, \text{B}_{0.02})\text{O}_4:\text{Eu}^{2+}_{0.1}$  and  $(\text{Sr}_{1-x}, \text{Zn}_x)_{0.9}(\text{Al}_{1.98}, \text{B}_{0.02})\text{O}_4:\text{Eu}^{2+}_{0.1}$  phosphors should overlap the emission band of the sites for the 460 nm emission. Figure 10 shows the emission spectrum for the  $(\text{Sr}_{0.1}, \text{Zn}_{0.9})_{0.9}(\text{Al}_{1.98}, \text{B}_{0.02})\text{O}_4:\text{Eu}^{2+}_{0.1}$  sample and the

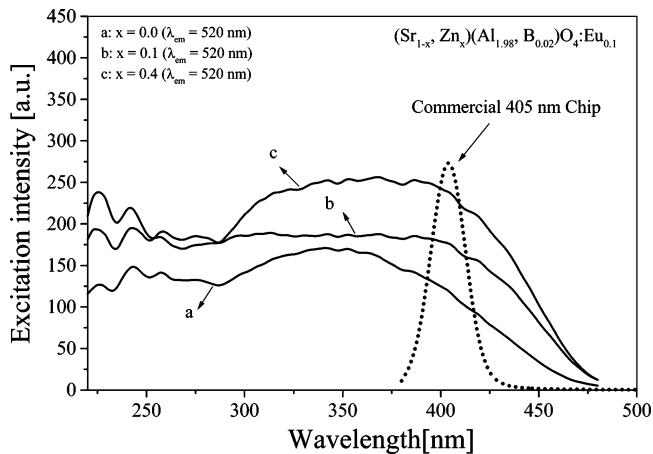


Figure 11. Excitation spectra of  $(\text{Sr}_{1-x}, \text{Zn}_x)(\text{Al}_{1.98}, \text{B}_{0.02})\text{O}_4:\text{Eu}^{2+}$  phosphors and emission spectrum of a commercial GaN chip.

excitation spectra of the  $\text{Sr}_{0.9}(\text{Al}_{1.98}, \text{B}_{0.02})\text{O}_4:\text{Eu}^{2+}_{0.1}$  and  $(\text{Sr}_{0.6}, \text{Zn}_{0.4})_{0.9}(\text{Al}_{1.98}, \text{B}_{0.02})\text{O}_4:\text{Eu}^{2+}_{0.1}$  samples. It was clear that the excitation spectra of both  $\text{Sr}_{0.9}(\text{Al}_{1.98}, \text{B}_{0.02})\text{O}_4:\text{Eu}^{2+}_{0.1}$  and  $(\text{Sr}_{0.6}, \text{Zn}_{0.4})_{0.9}(\text{Al}_{1.98}, \text{B}_{0.02})\text{O}_4:\text{Eu}^{2+}_{0.1}$  well overlap with the 460 nm emission for the  $(\text{Sr}_{0.1}, \text{Zn}_{0.9})_{0.9}(\text{Al}_{1.98}, \text{B}_{0.02})\text{O}_4:\text{Eu}^{2+}_{0.1}$  sample. From the results so far achieved, we concluded that the substitution of zinc atoms into the Sr sites produces new blue emission sites that play the role of sensitizer for the energy transfer, which consequently results in a large enhancement in the luminescence intensity of  $(\text{Sr}_{1-x}, \text{Zn}_x)_{0.9}(\text{Al}_{1.98}, \text{B}_{0.02})\text{O}_4:\text{Eu}^{2+}_{0.1}$ , wherein  $x$  is lower than 0.6.

Figure 11 shows the excitation spectra of  $(\text{Sr}_{1-x}, \text{Zn}_x)_{0.9}(\text{Al}_{1.98}, \text{B}_{0.02})\text{O}_4:\text{Eu}^{2+}_{0.1}$  phosphor. The emission spectrum of the commercial GaN chip ( $\lambda_{\text{max}} = 405$  nm) was also displayed in Figure 11. As shown in Figure 11, the addition of zinc atoms greatly increased the excitation intensity of the  $\text{Sr}_{0.9}(\text{Al}_{1.98}, \text{B}_{0.02})\text{O}_4:\text{Eu}^{2+}_{0.1}$  phosphor, especially in the wavelength range from 370 to 450 nm. Given that the phosphor for the UV LED application is required to have good excitation in the wavelength range from 380 to 420 nm, the optimized  $(\text{Sr}_{0.6}, \text{Zn}_{0.4})_{0.9}(\text{Al}_{1.98}, \text{B}_{0.02})\text{O}_4:\text{Eu}^{2+}_{0.1}$  phosphor can be successfully used as a promising green phosphor.

#### 4. Conclusion

We have prepared  $(\text{Sr}_{1-x}, \text{Zn}_x)_{1-y}(\text{Al}_{1.98}, \text{B}_{0.02})\text{O}_4:\text{Eu}^{2+}_y$  phosphor with spherical shape by spray pyrolysis and investigated the luminescent properties. Pure monoclinic  $\text{SrAl}_2\text{O}_4$  phase was formed until the post-treatment temperature was increased up to 1200 °C. The  $\text{Sr}_4\text{Al}_{14}\text{O}_{25}$  phase appeared as a minor phase when the temperature was over 1300 °C. As a result, the intensity of the green emission at 520 nm had the maximum value at 1200 °C. The concentration quenching of the emission intensity was observed when the  $\text{Eu}^{2+}$  content was 10 mol %. It was confirmed that the  $\text{B}^{3+}$  codoping is very helpful and necessary to enhance the luminescence intensity, but the large content accelerated the formation of  $\text{Sr}_4\text{Al}_{14}\text{O}_{25}$  phase and thereby reduced the emission intensity. It was found that the substitution of Zn atoms instead of the strontium produced a new blue (460 nm) emission site that was stable at ambient temperature and appeared to play the role of sensitizer for the energy transfer.

Consequently, the Zn substitution of less than 50% greatly improved the luminescence efficiency, especially in the excitation wavelength range from 380 to 420 nm. Therefore, the optimized phosphor (Sr<sub>0.6</sub>, Zn<sub>0.4</sub>)<sub>0.9</sub>(Al<sub>1.98</sub>, B<sub>0.02</sub>):Eu<sup>2+</sup><sub>0.1</sub> was expected to be used as a green phosphor for ultraviolet LEDs.

**Acknowledgment.** This work was supported by the Information Display R&D Center, one of the 21st Century Frontier R&D Program funded by the Ministry of Commerce, Industry and Energy of Korea.

CM060003W